Advances in Robotics Research, *Vol. 1, No. 1 (2014) 061-079*
DOI: http://dx.doi.org/10.12989/arr.2014.1.1.061

Dynamic characterisation of a two-link flexible manipulator: theory and experiments

M. Khairudin[1], Z. Mohamed[*2], A.R. Husain[2] and R. Mamat[2]

[1]*Department of Electrical Engineering, Universitas Negeri Yogyakarta, Indonesia*
[2]*Faculty of Electrical Engineering, Universiti Teknologi Malaysia, Malaysia*

(Received June 17, 2013, Revised October 30, 2013, Accepted November 1, 2013)

Abstract. This paper presents theoretical and experimental investigations into the dynamic modelling and characterisation of a two-link flexible manipulator incorporating payload. A planar two-link flexible manipulator that moves in a horizontal plane is considered. A dynamic model of the system is developed using a combined Euler-Lagrange and assumed mode methods, and simulated using Matlab. Experiments are performed on a lab-scaled two-link flexible manipulator for validation of the dynamic model and characterisation of the system. Two system responses namely hub angular position and deflection responses at both links are obtained and analysed in time and frequency domains. The effects of payload on the dynamic characteristics of the flexible manipulator are also studied and discussed. The results show that a close agreement between simulation and experiments is achieved demonstrating an acceptable accuracy of the developed model.

Keywords: assumed mode; dynamic characterisation; experiment; modelling; two-link flexible manipulator

1. Introduction

Flexible manipulators have several advantages over rigid robots: they require less material, lighter in weight, consume less power, require smaller actuators, more manoeuvrable and transportable, have less overall cost and higher payload to robot weight ratio. These types of robots are used in a wide spectrum of applications starting from simple pick and place operations of an industrial robot to micro-surgery, maintenance of nuclear plants and space robotics (Dwivedy and Eberhard 2006). For practical applications, two-link flexible manipulators are preferred as they provide more flexibility in their applications. However, control of flexible manipulators to maintain accurate positioning is an extremely challenging. The complexity of the problem increases dramatically for a two-link flexible manipulator as the system is a class of multi-input multi-output (MIMO) systems and several other factors such as coupling between both links and effects of vibration between both links have to be considered. Moreover, the dynamic behaviour of the manipulator is significantly affected by payload variations (Nikolakopoulos and Tzes 2010).

The main goal of modelling of a two-link flexible manipulator is to achieve an accurate model representing the actual system behaviour. It is important to recognise the flexible nature and

*Corresponding author, Ph.D., E-mail: zahar@fke.utm.my

 ISSN: 2287-4976 (Print), 2287-4984 (Online)

dynamic characteristics of the system and construct a suitable mathematical framework. Modelling of a single-link flexible manipulator has been widely established. Various approaches have been developed which can mainly be divided into two categories: the numerical analysis approach and the assumed mode method (AMM). The numerical analysis methods that are utilised include finite difference and finite element methods (Martins *et al*. 2003, Tokhi and Mohamed 1999). Besides, several other methods have also been studied. These include a particle swarm optimisation algorithm (Alam and Tokhi 2007) and extended Hamilton's principle and generalised Galerkin's method (Pratiher and Dwivedy 2007). Jun Wu *et al*. (2013) have also presented a technique to study dynamic characteristics of a dynamic system such as a parallel manipulator.

Similar to the case of a single-link manipulator, the finite element method and AMM have also been investigated for modelling of a two-link flexible robot manipulator. Yang and Sadler (1990) and Dogan and Istefanopulos (2007) have developed the finite element models to describe the deflection of a planar two-link flexible robot manipulator. De Luca and Siciliano (1991) have utilised the AMM to derive a dynamic model of multilink flexible robot arms limiting to the case of planar manipulators with no torsional effects. Subudhi and Morris (2002) have also presented a systematic approach for deriving the dynamic equations for *n*-link manipulator where two-homogenous transformation matrices are used to describe the rigid and flexible motions respectively.

However, most of investigations on modelling and dynamic characterisation of a two-link flexible manipulator were based on simulation exercises with limited experimental validations. It is important and desirable for control purposes to validate the simulation results with an actual system. Moreover, not much work on experimental validation of dynamic characteristics of a two-link flexible manipulator with payload been reported. This paper presents theoretical and experimental investigations into dynamic modelling and characterisation of a two-link flexible manipulator incorporating payload. A two-link flexible manipulator that moves in a horizontal plane is considered. A payload is attached at the end-point of the second-link whereas hub inertias are considered at the actuator joints. Simulation and analysis of the dynamic model is performed within Matlab and Simulink environment. System responses namely hub angular position and deflection are evaluated in both time and frequency domains. Moreover, the work investigates the effects of varying payload on the dynamic characteristics of the system. Experimental exercises are performed on a lab-scale two-link flexible manipulator for validation of the dynamic model and characterisation of the system. This is carried out by comparing the simulation and experimental results both in time and frequency domains. The work presented forms the basis of design and development of suitable control strategies for two-link flexible manipulator systems.

2. The two-link flexible manipulator system

Fig. 1 shows the experimental two-link flexible manipulator considered in this work. The system was designed for experimental verification of modelling and controller designs involving two-link flexible manipulators. The experimental rig used in this work consists of three main parts: a two-link flexible arm, measuring devices and a processor. The flexible links are constructed using a piece of thin aluminium with specifications as given in Table 1. The experimental rig is equipped with a precision interface circuit, PCI6221 used as a multifunctional data acquisition card for synchronisation of input and output signals from the hardware to a computer. The card has two 16-bit analogue outputs and 24 digital input/output ports.

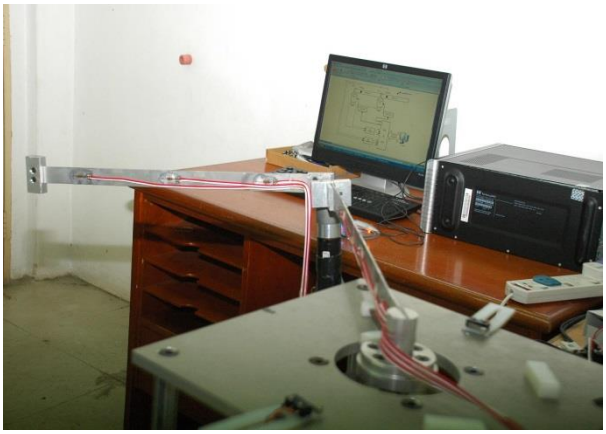

Fig. 1 The experimental two-link flexible manipulator

Table 1 Parameters of a two-link flexible manipulator

Symbol	Parameter	Link-1	Link-2	Unit
M_{L1}, M_{L2}	Mass of link	0.08	0.05	kg
ρ	Mass density	2666.67	2684.56	kgm^{-1}
EI	Flexural rigidity	1768.80	597.87	Nm^2
J_h	Motor and hub inertia	1.46×10^{-3}	0.60×10^{-3}	kgm^2
M_p	Payload mass maximum	-	0.1	kg
J_p	Payload inertia maximum	-	0.5×10^{-3}	kgm^2
l	Length of link	0.5	0.5	m
	Width of link	0.03	0.025	m
	Thickness of link	2×10^{-3}	1.49×10^{-3}	m
J_o	Moment of inertia	5×10^{-3}	3.125×10^{-3}	kgm^2
M_{h2}	Mass of the centre rotor	-	0.155	kg

The measuring devices used in this work are shaft encoders at the motors and strain gauges placed along the arms. Two encoders, HEDL-5540 and HEDS-5540 (Maxon 2003) with 500 counts per turn are used to measure the angular positions of link-1 and link-2 respectively. A precision interface circuit consisting of PCIQUAD04 with 4 input channels has been constructed for measurement and interfacing with real-time system. On the other hand, the strain gauges are used for measurement of deflections of the links. Strain gauges use a wheat-stone bridge circuit to convert the resistance change to voltage output for strain measurement (Tokyo Sokki 1996). For the two-link flexible manipulator, two strain gauges are placed at 10 cm from the hubs of both links as these locations provide feasible deflection response.

In this work, Matlab Real-Time toolbox is used for real-time interfacing and control of the system. The processor used for this experimental rig is Pentium (R) Dual CPU E2140 with 1.60 GHz speed. Data acquisition and control are accomplished through utilisation of PCI6221 I/O board that provides a direct interface between the processor, actuators and sensors through signal conditioning circuits SCC-AI for analogue input, SCC-AO for analogue output and SCC-SG for

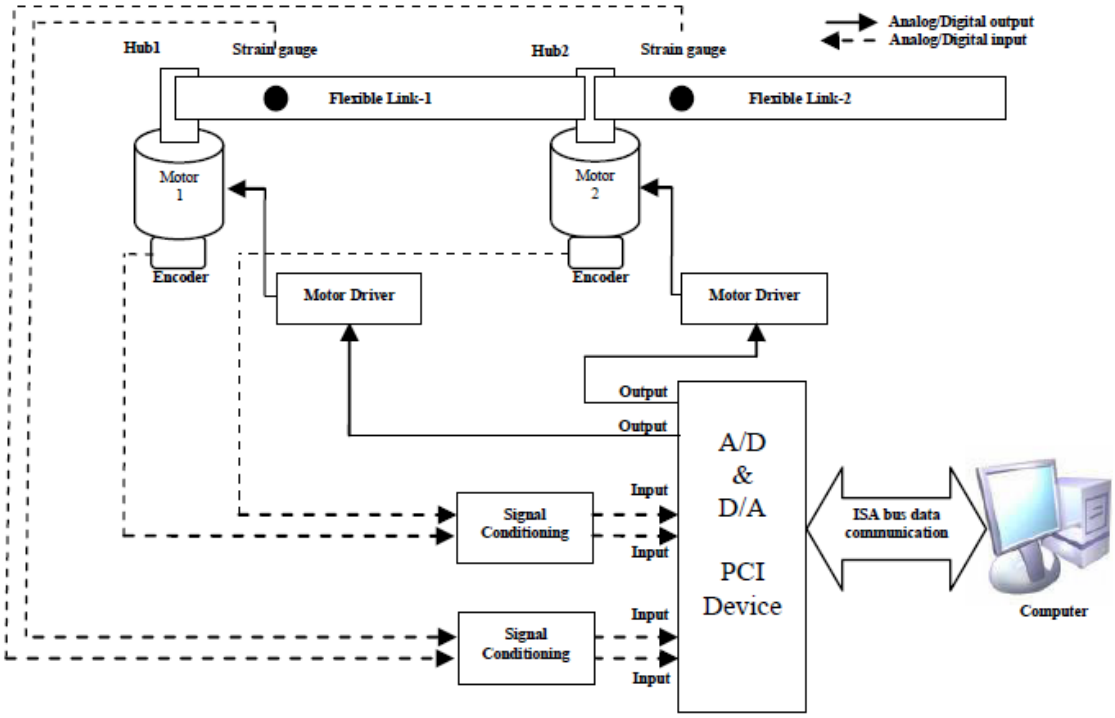

Fig. 2 Schematic diagram of an experimental rig

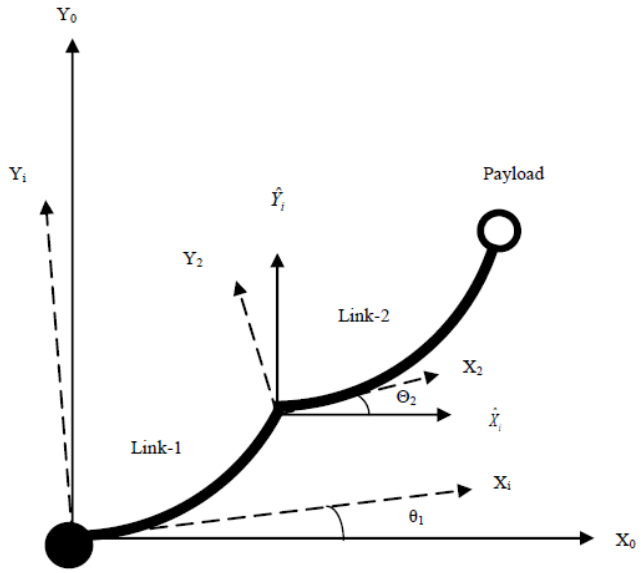

Fig. 3 Structure of a two-link flexible manipulator

strain gauges. The experimental rig requires two-analogue outputs for both motors and four analogue inputs from the encoders and strain gauges for both links. Fig. 2 shows the schematic

diagram of the experimental rig.

Fig. 3 shows a structure of a two-link flexible manipulator considered in these investigations. The links are cascaded in a serial fashion and are actuated by rotors and hubs with individual motors. The *i*th link has length l_i with uniform mass density per unit length ρ_i. The first link is clamped at the rotor of the first motor whereas the second motor is attached at the tip of the first link. *E* and *I* represent Young modulus and area moment of inertia of both links respectively. A payload is attached at the end-point of link-2. X_0Y_0 is the inertial co-ordinate frame, X_iY_i is the rigid body coordinate frame associated with the *i*th link and $\hat{X}_i\hat{Y}_i$ is the moving coordinate frame. θ_1 and θ_2 are the angular positions and $v_i(x_i,t)$ is the transverse component of the displacement vector. M_n is an inertial payload mass with inertia J_n at the end-point of link-2. The physical parameters of the two-link flexible manipulator system considered in this study are shown in Table 1. M_{h2} is the mass considered at the second motor which is located in between both links, J_{hi} is the inertia of the *i*th motor and hub. The input torque, $\tau_i(t)$ is applied at each motor and G_i is the gear ratio for the *i*th motor. Both links and motors are considered to have the same dimensions.

3. Dynamic modelling

This section focuses on the development of a combined Euler-Lagrange and AMM simulation algorithm characterising the dynamic behaviour of the two-link flexible manipulator system. The description of kinematics is developed for a chain of *n* serially connected flexible links. Considering revolute joints and motion of the manipulator on a two-dimensional plane, the rigid transformation matrix, A_i, from $X_{i-1}Y_{i-1}$ to $X_i Y_i$ can be written as (De Luca and Siciliano 1991, Subudhi and Morris 2002)

$$A_i = \begin{bmatrix} \cos(\theta_i) & -\sin(\theta_i) \\ \sin(\theta_i) & \cos(\theta_i) \end{bmatrix} \tag{1}$$

The elastic homogenous transformation matrix, E_i, due to the deflection of the link *i* can be obtained as

$$E_i = \begin{bmatrix} 1 & -\dfrac{\partial \upsilon_i(x_i,t)}{\partial x_i}\Big|_{x_i=l_i} \\ \dfrac{\partial \upsilon_i(x_i,t)}{\partial x_i}\Big|_{x_i=l_i} & 1 \end{bmatrix} \tag{2}$$

where $\upsilon_i(x_i,t)$ is the bending deflection of the *i*th link at a spatial point x_i ($0 \le x_i \le l_i$). The global transformation matrix T_i transforming co-ordinates from X_0Y_0 to $X_i Y_i$ follow a recursion as

$$T_i = T_{i-1}E_{i-1}A_i = \hat{T}_{i-1}A_i; \quad \hat{T}_0 = I \tag{3}$$

where *I* is an identity matrix. Let ${}^i r_i(x_i) = \begin{Bmatrix} x_i \\ \upsilon_i(x_i,t) \end{Bmatrix}$ be the position vector that describes an

arbitrary point along the *i*th deflected link with respect to its local coordinate frame (X_iY_i) and ${}^0r_i$ be the same point referring to X_0Y_0. The position of the origin of $X_{i+1}Y_{i+1}$ with respect to X_iY_i is given by

$$ {}^i p_{i+1} = {}^i r_i(l_i) \tag{4}$$

where ${}^0 p_i$ is its absolute position with respect to X_0Y_0. Using the global transformation matrix, ${}^0r_i$ and ${}^0 p_i$ can be written as

$$ {}^0r_i = {}^0p_i + T_i\, {}^i r_i; \qquad {}^0 p_{i+1} = {}^0p_i + T_i\, {}^i p_{i+1} \tag{5}$$

To derive the dynamic equations of motion of a two-link flexible manipulator, the total energies associated with the manipulator system needs to be computed using the kinematics formulations. The total kinetic energy of the manipulator is given by

$$ C = C_R + C_L + C_{PL} \tag{6}$$

where C_R, C_L and C_{PL} are the kinetic energies associated with the rotors, links and the hubs, respectively. The kinetic energy of the *i*th rotor can be obtained as

$$ C_{Ri} = \frac{1}{2} G_i^{\,2} J_{hi} \dot{\alpha}_i^{\,2} \tag{7}$$

where $\dot{\alpha}_i$ is the angular velocity of the rotor about the *i*th principal axis. Moreover, the kinetic energy of a point $r_i(x_i)$ on the *i*th link can be written as

$$ C_{Li} = \frac{1}{2} \rho_i \int_0^{l_i} {}^0\dot{r}_i^{\,T}(x_i)\, {}^0\dot{r}_i(x_i)\, dx_i \tag{8}$$

where ${}^0\dot{r}_i(x_i)$ is the velocity vector. The velocity vector can be computed by taking the time derivative of Eq. (5)

$$ {}^0\dot{r}_i(x_i) = {}^0\dot{p}_i + \dot{T}_i\, {}^i r_i(x_i) + T_i\, {}^i\dot{r}_i(x_i) \tag{9}$$

where ${}^0\dot{p}_i$ can be determined by using Eqs. (4) and (5) along with

$$ {}^i\dot{p}_{i+1} = {}^i\dot{r}_i(l_i) \tag{10}$$

Furthermore, the time derivative of the global transformation matrix $\dot{T}_i$ can be recursively calculated from (De Luca and Siciliano 1991)

$$ \dot{T}_i = \dot{\hat{T}}_{i-1} A_i + \dot{\hat{T}}_{i-1} \dot{A}_i, \qquad \dot{\hat{T}}_i = T_i E_i + T_i \dot{E}_i \tag{11}$$

Computation of $\dot{A}_i$ and $\dot{E}_i$ in Eq. (11) can be performed as follows

$$ \dot{A}_i = S A_i \dot{\theta}_i \quad \text{and} \quad \dot{E}_i = S \frac{\partial \dot{\upsilon}_i}{\partial x_i}\Big|_{x_i = l_i}, \quad S = \begin{bmatrix} 0 & -1 \\ 1 & 0 \end{bmatrix} \tag{12}$$

Evaluation of the transpose and derivative of transpose terms of the velocity vector in Eq. (8) can be accomplished by utilising the following identities

$$A_i^T A_i = E_i^T E_i = S^T S + I \quad \text{and} \quad E_i^T \dot{E}_i = (I\upsilon_i'(l_i,t) + S)\dot{\upsilon}_i'(l_i,t) \tag{13}$$

$$A_i^T \dot{A}_i = S\dot{\theta}_i \tag{14}$$

where I is the identity matrix of appropriate dimensions. Once, the kinetic energy associated with the ith link is obtained, the kinetic energy of all the n links can thus be found as

$$C_L = \sum_{i=1}^{n} \frac{1}{2} \rho_i \int_0^{l_i} {}^0\dot{r}_i^T(x_i)\,{}^0\dot{r}_i(x_i)dx_i \tag{15}$$

As shown in Fig. 3 and the kinematics formulation described previously, the kinetic energy associated with the payload can be written as

$$C_{PL} = \frac{1}{2} M_p \dot{p}_{n+1}^T \dot{p}_{n+1} + \frac{1}{2} I_P (\dot{\Omega}_n + \dot{\upsilon}_n'(l_n))^2 \tag{16}$$

where $\dot{\Omega}_n = \sum_{i=1}^{n} \theta_j + \sum_{k=1}^{n-1} \dot{\upsilon}_k'(l_k)$; n being the link number, prime and dot represent the first derivatives with respect to spatial variable x and time, respectively.

The total potential energy of the system due to the deformation of the link i by neglecting the effects of the gravity can be written as

$$U = \sum_{i}^{n} \frac{1}{2} \int_0^{l_i} (EI)_i \left(\frac{d^2 \upsilon_i(x_i)}{dx_i^2} \right)^2 dx_i \tag{17}$$

where EI is the flexural rigidity of the system. The dynamics of the link at an arbitrary spatial point x_i along the link at an instant of time t can be written using Euler-Beam theory as

$$(EI)_i \frac{\partial^4 \upsilon_i(x_i,t)}{\partial x_i^4} + \rho_i \frac{\partial^2 \upsilon_i(x_i,t)}{\partial t^2} = 0 \tag{18}$$

On the other hand, bending deflections $\upsilon_i(x_i,t)$ can be expressed as a superposition of mode-shapes and time dependent modal displacements as

$$\upsilon_i(x_i,t) = \sum_{j=1}^{n_m} \phi_{ij}(x_i) q_{ij}(t) \tag{19}$$

where $q_{ij}(t)$ and $\phi_{ij}(x_i)$ are the jth modal displacement and jth mode shape function for the ith link. The solution of Eq. (19) is in the form of

$$\phi_{ij}(x_i) = m_i[\cos(\beta_{ij} x_i) - \cosh(\beta_{ij} x_i + \gamma_{ij}(\sin(\beta_{ij} x_i) - \sinh(\beta_{ij} x_i))] \tag{20}$$

where m_i is the mass of link *i* and γ_{ij} is given as

$$\gamma_{ij} = \frac{\sin\beta_{ij} - \sinh\beta_{ij} + \dfrac{M_{L_i}\beta_{ij}}{\rho_i}(\cos\beta_{ij} - \cosh\beta_{ij})}{\cos\beta_{ij} + \cosh\beta_{ij} - \dfrac{M_{L_i}\beta_{ij}}{\rho_i}(\sin\beta_{ij} - \sinh\beta_{ij})} \tag{21}$$

and β_{ij} is the solution of the following equation

$$\begin{aligned} &1 + \cosh\beta_{ij}l_i\cos\beta_{ij}l_i - \frac{M_{L_i}\beta_{ij}}{\rho_i}(\sin\beta_{ij}l\cosh\beta_{ij}l_i - \cos\beta_{ij}l_i\sinh\beta_{ij}l_i) - \frac{J_{L_i}\beta_{ij}^{\ 3}}{\rho_i} \\ &(\sin\beta_{ij}l_i\cosh\beta_{ij}l + \cos\beta_{ij}l_i\sinh\beta_{ij}l_i) + \frac{M_{L_i}J_{L_i}\beta_{ij}^{\ 4}}{\rho_i^{\ 2}}(1 - \cos\beta_{ij}l_i\cosh\beta_{ij}l_i) = 0 \end{aligned} \tag{22}$$

Subsequently, the natural frequency for the *j*th mode and *i*th link, ω_{ij}, is determined from the following expression (Tao Fan 2007)

$$\omega_{ij} = \beta_{ij}^{\ 2}\sqrt{\frac{(EI)_i}{\rho_i}} \tag{23}$$

In this work, the dynamic model of the system incorporating payload is investigated. In this case, the effectiveness masses at the end of the individual links (M_{L1} for link-1 and M_{L2} for link-2) are set as

$$\begin{aligned} M_{L1} &= m_2 + m_{h2} + M_p \\ M_{L2} &= M_p \end{aligned} \tag{24}$$

and the effectiveness inertia of the individual links (J_{L1} for link-1 and J_{L2} for link-2) are

$$\begin{aligned} J_{L1} &= J_{o2} + J_{h2} + J_p + M_p l_2^2 \\ J_{L2} &= J_p \end{aligned} \tag{25}$$

where m_2 is the mass of link-2 and J_{o2} is the joint inertia of link-2 about joint-2 axis.

The co-ordinate vector consists of link positions, (θ_1, θ_2) and modal displacements (q_{11}, q_{12}, q_{21}, q_{22}). The force vector is $F = \{\tau_1, \tau_2, 0, 0, 0, 0\}^{\mathrm{T}}$, where τ_1 and τ_2 are the torques applied at the hubs of link-1 and link-2, respectively. The dynamic equations of motion of a two-link flexible manipulator can be derived utilising the Euler–Lagrange's equations with the Langrangian, $L = C - U$. With i = 1 and 2 and j = 1 and 2, the equation can be obtained as

$$\frac{\partial}{\partial t}\left(\frac{\partial L}{\partial \dot{\theta}_i}\right) - \frac{\partial L}{\partial \theta_i} = \tau_i \tag{26}$$

and

$$\frac{\partial}{\partial t}\left(\frac{\partial L}{\partial \dot{q}_{ij}}\right)-\frac{\partial L}{\partial q_{ij}}=0 \tag{27}$$

Considering the damping, the desired dynamic equations of motion of a two-link flexible manipulator can be obtained as

$$M(\theta,q)\begin{Bmatrix}\ddot{\theta}\\ \ddot{q}\end{Bmatrix}+\begin{Bmatrix}f_1(\theta,\dot{\theta})\\ f_2(\theta,\dot{\theta})\end{Bmatrix}+\begin{Bmatrix}g_1(\theta,\dot{\theta},q,\dot{q})\\ g_2(\theta,\dot{\theta},q,\dot{q})\end{Bmatrix}+\begin{Bmatrix}0\\ D\dot{q}\end{Bmatrix}+\begin{Bmatrix}0\\ Kq\end{Bmatrix}=\begin{Bmatrix}\tau\\ 0\end{Bmatrix} \tag{28}$$

where f_1 and f_2 are the vectors containing terms due to coriolis and centrifugal forces, M is the mass matrix and g_1 and g_2 are the vectors containing terms due to the interactions of the link angles and their rates with the modal displacements. K is the diagonal stiffness matrix which the values of $\omega_{ij}{}^2 m_i$ and D is the passive structural damping as

$$K = diag\left\{0,\, 0,\, \omega_{11}^2 * m_1,\, \omega_{12}^2 * m_1,\, \omega_{21}^2 * m_2,\, \omega_{22}^2 * m_2\right\} \tag{29}$$

$$D_i = 0.1\sqrt{K_i}\,, i = 3,\ldots,6 \tag{30}$$

4. Implementation and results

In this section, simulation and experimental results of response of the two-link flexible manipulator are presented in the time and frequency domains. A bang-bang signal with amplitude of ±0.15 V as shown in Fig. 4 is used as an input voltage applied at the hub of link-1 of the manipulator. The same form of signal with amplitude of ±0.03 V is used as the input signal for link-2. A bang-bang signal is utilised as the signal has a positive (acceleration) and negative (deceleration) period allowing the manipulator to, initially, accelerate and then decelerate and eventually stop at a target location. Two system responses namely the hub angular positions and deflections at 10 cm from the hubs of both links with the frequency response of the deflections are obtained and evaluated. Moreover, the effects of varying payload on system behaviour are also studied. For these investigations, the system without payload, and the system with payloads of 0.05 kg and 0.1 kg are considered.

Simulation of the developed dynamic model was implemented within the Matlab and Simulink environment on Intel Pentium 1.60 GHz and 1.99 GB RAM. The system responses are monitored for duration of 5 s, and the results are recorded with a sampling time of 10 ms. Experiments were conducted using the experimental rig for verification of the simulation results of the dynamic model. In both exercises, single-switch bang-bang input voltages with the same parameters were used. The angular position and deflection responses were measured and the corresponding responses in the frequency domains were obtained. For evaluation of the time response of the angular position, settling time and overshoot of the response are obtained. On the other hand for evaluation of the frequency response, resonance frequencies of the deflection response are examined. Finally, both simulation and experimental results are compared to examine the accuracy of the developed dynamic model.

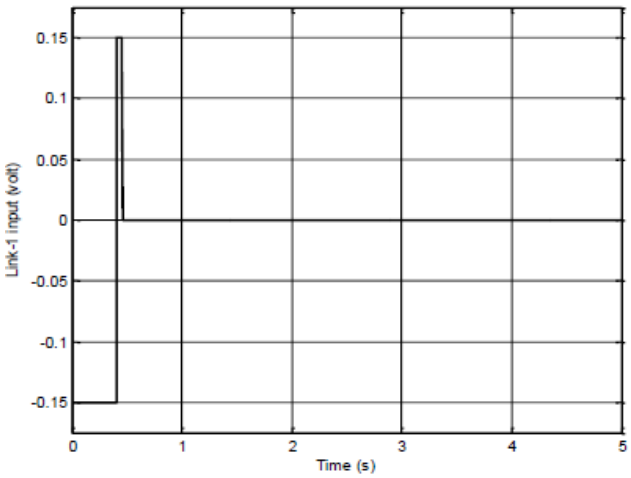

Fig. 4 Structure of a two-link flexible manipulator

Table 2 Relation between payloads and specifications of angular positions of the flexible manipulator (sim: simulation; exp: experiment)

Load (kg)	Link-1				Link-2			
	Settling time (s)		Overshoot (%)		Settling time (s)		Overshoot (%)	
	Sim	Exp	Sim	Exp	Sim	Exp	Sim	Exp
0.00	0.85	0.88	2.05	0.11	0.75	0.63	2.77	0.13
0.05	1.04	0.95	2.16	0.13	0.85	0.65	2.89	0.16
0.10	1.08	1.01	2.37	0.17	0.91	0.67	3.28	0.22

4.1 The system without payload

Fig. 5 shows simulation and experimental results of the angular position responses of the two-link flexible manipulator without payload for both links. Both simulation and experimental results show similar results for link-1 and link-2, where steady-state angular position levels of -0.50 rad and 0.35 rad were achieved respectively. The transient response specifications of the angular position for both links with the simulation and experiment are summarised in Table 2.

Fig. 6 shows simulation and experimental results of the deflection responses of link-1 and link-2. It is noted that the simulation and experimental responses for both links eventually converge to zero. With the simulation results, the maximum magnitudes of the responses were 9.8 mm and 5.2 mm for link-1 and link-2 respectively. On the other hand with the actual system, the maximum magnitudes were 10.3 mm and 5.5 mm. Fig. 7 shows the frequency responses of the deflection responses obtained with simulation and experimental exercises. These were obtained by transforming the time response into the frequency domain using Fast Fourier Transform. The results show that the system dynamic behaviour is characterised by the first two modes of vibrations. Both simulation and experimental results show that the vibration occurs at 13.7 Hz and 33.3 Hz for link-1 and 15.6 Hz and 33.3 Hz for link-2. Table 3 summarises resonance frequencies of the deflection response for link-1 and link-2 with simulation and experiment. The responses

Table 3 Relation between payloads and resonance frequencies of the flexible manipulator (sim: simulation; exp: experiment)

Load (kg)	Link-1				Link-2			
	Mode-1 (Hz)		Mode-2 (Hz)		Mode-1 (Hz)		Mode-2 (Hz)	
	Sim	Exp	Sim	Exp	Sim	Exp	Sim	Exp
0.00	13.7	13.7	33.3	33.3	15.6	15.6	33.3	33.3
0.05	8.1	11.0	27.5	29.4	12.0	13.7	27.4	25.5
0.10	7.8	7.8	27.1	25.5	11.7	11.7	27.1	23.5

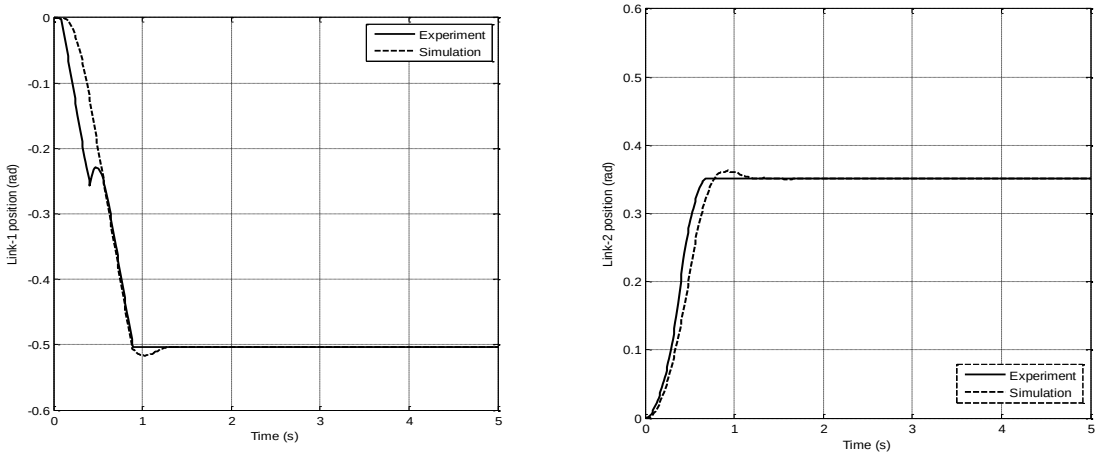

(a) Link-1 (b) Link-2

Fig. 5 Angular position response of the system without payload

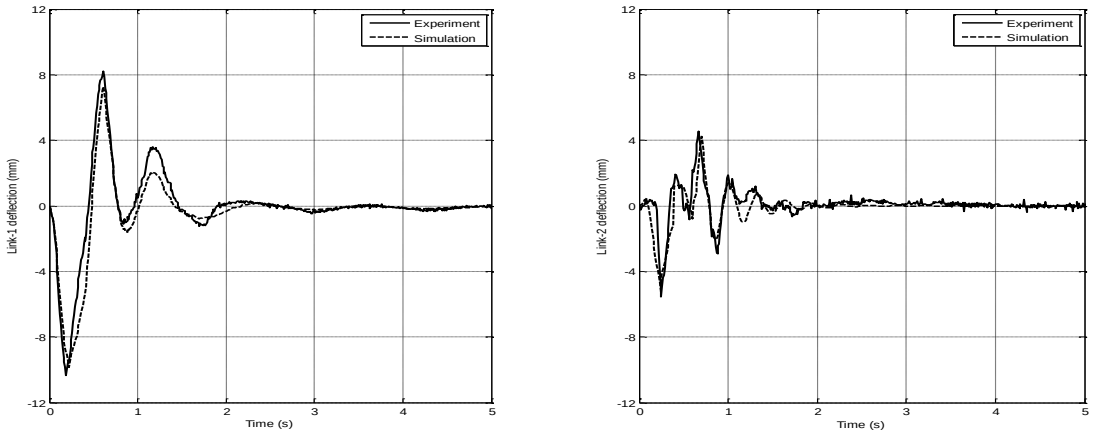

(a) Link-1 (b) Link-2

Fig. 6 Deflection response of the system without payload

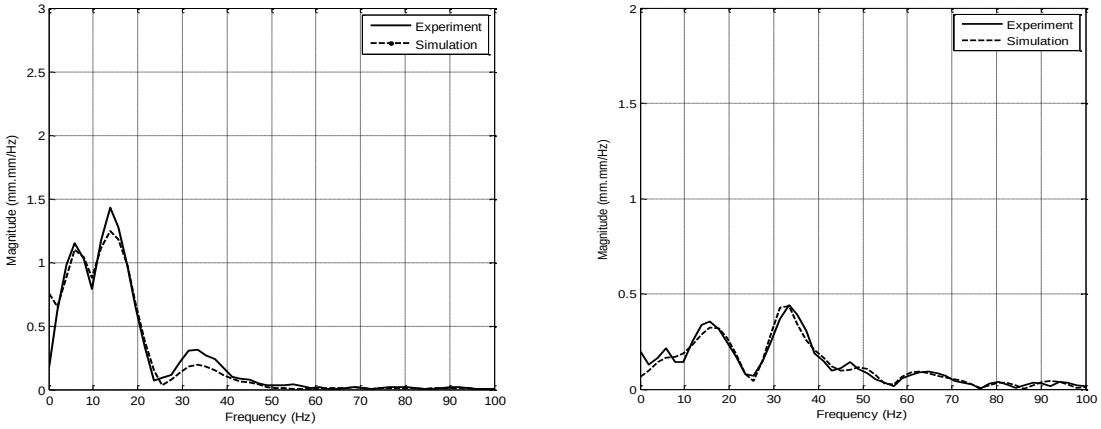

(a) Link-1 (b) Link-2

Fig. 7 Frequency response of deflection of the system without payload

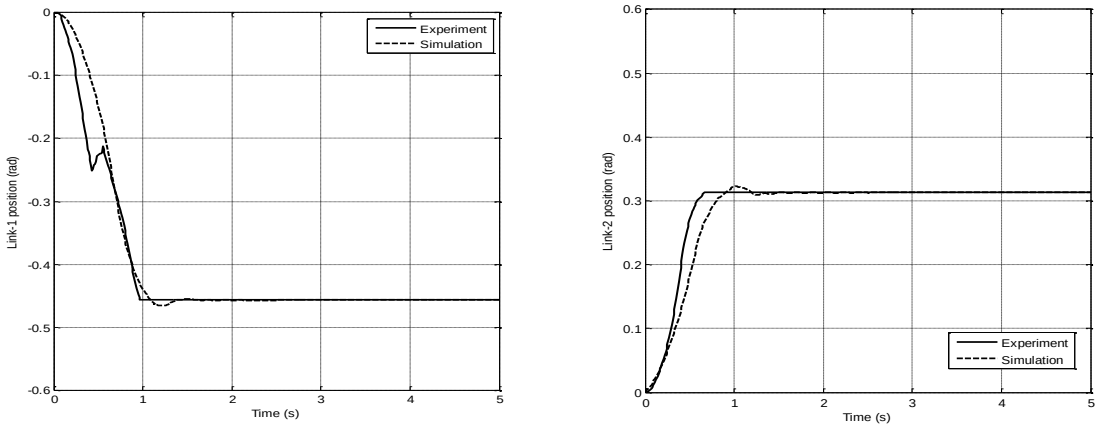

(a) Link-1 (b) Link-2

Fig. 8 Frequency response of deflection of the system without payload

reveal that significant vibrations occur during the movement of both links of the flexible manipulator.

4.2 The system with payload

To investigate the effects of payload on the dynamic characteristics of the system, a two-link flexible manipulator with various payloads was examined. Fig. 8 shows simulation and experimental results of angular position responses of the flexible manipulator with payload of 0.05 kg. The results with a payload of 0.1 kg are shown in Fig. 9. It is noted that the steady-state angular positions for link-1 and link-2 decrease with increasing payload. For simulations and experiments,

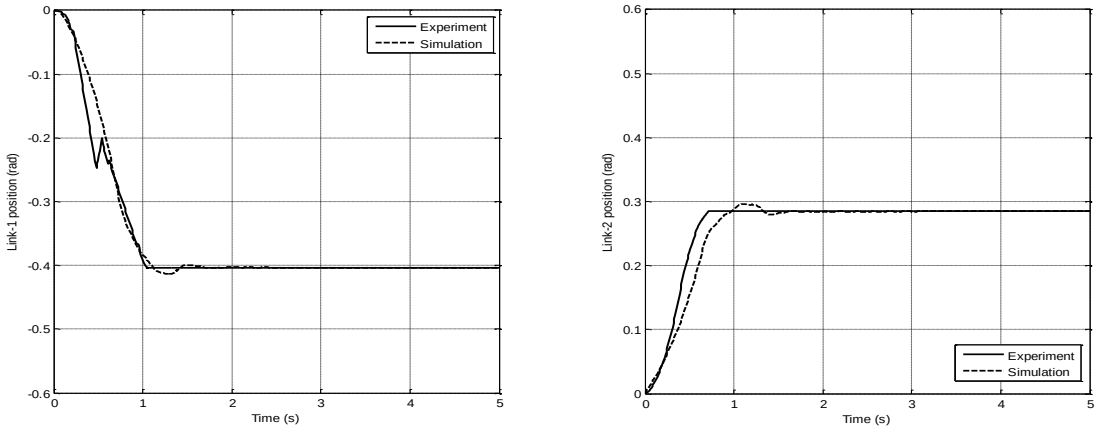

(a) Link-1 (b) Link-2

Fig. 9 Angular position response of the system with 0.1 kg payload

Table 4 Effects of payloads on maximum magnitudes of the deflection responses of the flexible manipulator

Payload (kg)	Maximum deflection of link-1 (mm)		Maximum deflection of link-2 (mm)	
	Simulation	Experiment	Simulation	Experiment
0.00	9.8	10.3	5.2	5.5
0.05	11.8	11.5	7.5	8.0
0.10	12.0	12.2	9.5	10.0

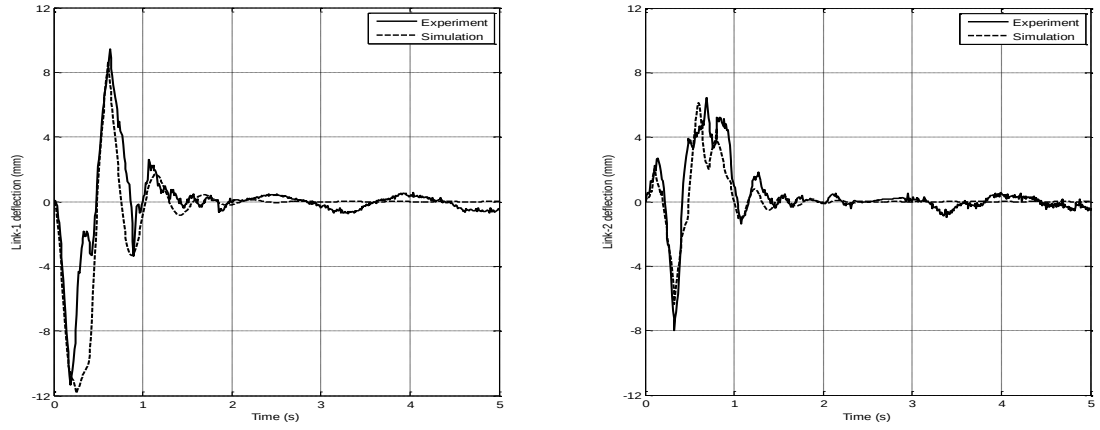

(a) Link-1 (b) Link-2

Fig. 10 Deflection response of the system with 0.05 kg payload

the steady-state angular position levels for link-1 were obtained as -0.46 rad and -0.40 rad for payloads of 0.05 kg and 0.1 kg respectively whereas for link-2, these were obtained as 0.31 rad and

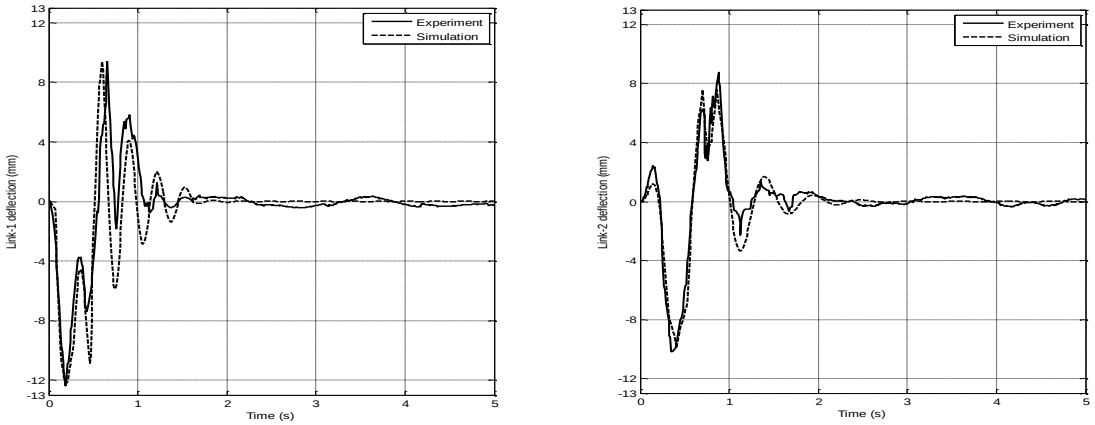

(a) Link-1 (b) Link-2

Fig. 11 Deflection response of the system with 0.1 kg payload

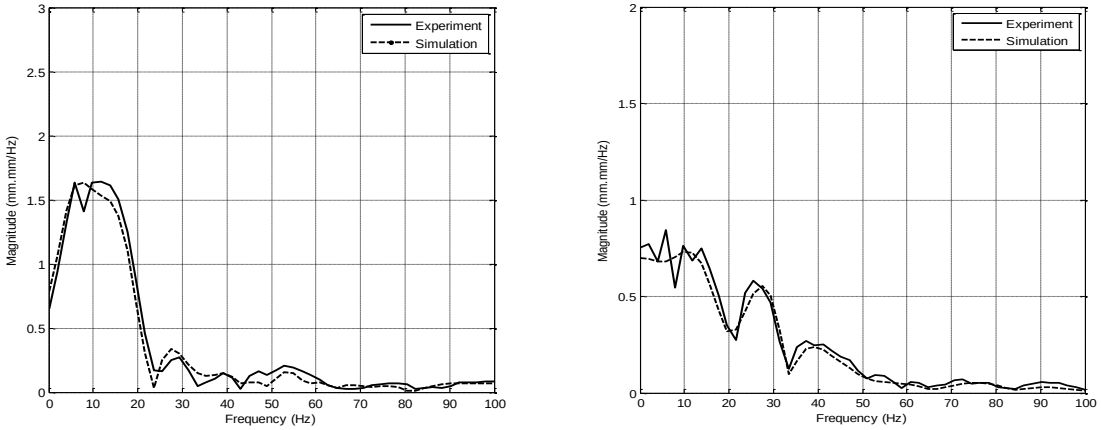

(a) Link-1 (b) Link-2

Fig. 12 Frequency response of deflection of the system with 0.05 kg payload

0.28 rad. The results also show that the transient responses of the system are affected by the variations of payloads. Table 2 summarises the settling time and overshoot of the angular position response with payloads of 0.05 kg and 0.1 kg. It is noted with increasing payload, the system exhibits higher settling times and overshoots for both links.

Figs. 10 and 11 show simulation and experimental results of the deflection responses for link-1 and link-2 of the flexible manipulator with payloads of 0.05 kg and 0.1 kg respectively. Similar to the results without payload, both the simulation and experimental responses eventually converge to zero. However, it is noted with increasing payloads, the magnitudes of vibration of the deflection increase for both links. Table 4 summarises the maximum magnitudes of the responses for link-1 and link-2 achieved with simulations and experiments. With the simulation results, the maximum

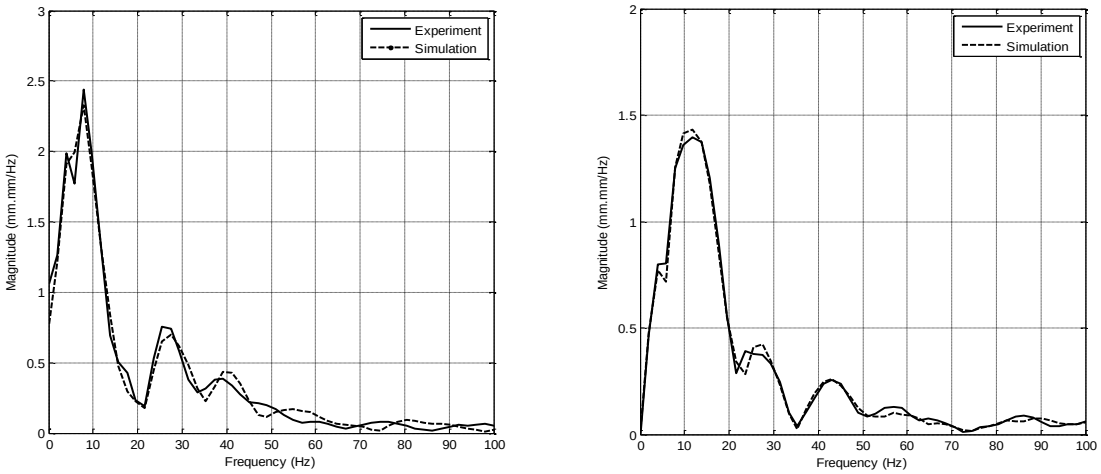

(a) Link-1 (b) Link-2

Fig. 13 Frequency response of deflection of the system with 0.1 kg payload

magnitudes of the responses increase by 20% and 22% for link-1 and 44% and 82% for link-2 for payloads of 0.05 kg and 0.1 kg respectively as compared to the response without payload. On the other hand with the experimental results, increments by 11% and 18% for link-1, and 45% and 81% for link-2 were noted. It is also noted that the response requires longer time to settle down to zero.

In this work, the frequency response of the deflection response is utilised to investigate the effects of payload on the dynamic behaviour of the system in the frequency domain. Figs. 12 and 13 show the frequency responses of the deflection obtained with simulation and experimental exercises with payloads of 0.05 kg and 0.1 kg respectively. The relations between the resonance frequencies of the deflection with payloads are summarised in Table 3. It is noted with simulation and experimental results, the resonance modes of vibration of the system shifts to lower frequencies with increasing payload. This implies that the manipulator oscillates at lower frequency rates than those without payload.

5. Model validation

Validation of a dynamic model for use in simulation and control is an important step before the model can be employed with confidence. In this work, the model validation is performed by comparing simulation and experimental results of the dynamic characteristics of the two-link flexible manipulator. It can be considered in two parts: time-domain validation that focuses on the time response of various system states to an input command, and frequency-domain validation, which involves the natural frequencies of the system. Time domain results show the effects of assumptions concerning the non-linear terms in the equations of motion.

Comparisons of the angular position and deflection responses of the system without payload (Figs. 5 and 6) reveal that the model provides a good prediction for both responses. These can be

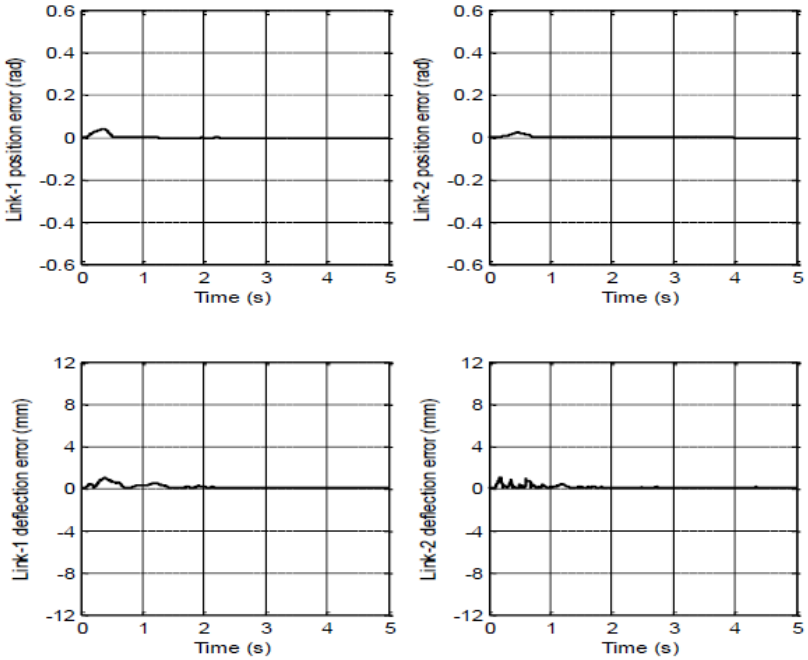

Fig. 14 Error between simulation and experimental results for the system without payload

observed with the characteristic and transient responses of the system where a close agreement between experimental and simulation results was obtained. However for the angular position response, a slight different is noted at the initial stage of link-1. This might be due to loading effects introduced by the second motor which is attached at the end of link-1. In addition, the gravity that might affect the motor is not included in the model used in the simulation. Nevertheless, in both cases, the manipulators reach similar steady-state levels of 0.41 rad and 0.35 rad. Fig. 14 shows errors between the simulation and experimental results of the responses for link-1 and link-2. It is further revealed that a reasonable close agreement was achieved as the maximum errors are negligible small. For the frequency-domain validation, comparisons of the resonance frequencies for link-1 and link-2 (Fig. 7 and Table 3) show exact matching of simulation and experimental results. Matching of natural frequencies is a good indication of accurately modelled mass and stiffness properties.

Comparisons of the angular position responses (Figs. 8 and 9) and the deflection responses (Figs. 10 and 11) of the manipulator with payloads of 0.05 kg and 0.1 kg also reveal similar results as the system without payload. The dynamic model provides a satisfactory prediction of the actual two-link flexible manipulator for both links. For the angular position responses, despite of a slight different at the initial stage of the response, the same steady-state levels were achieved for both links. As expected, the steady-state levels of the angular position decrease with increasing payload. Table 3 shows that the simulation algorithm provides a close characteristic behaviour of the transient response of experimental rig with increasing payload. In this case, both simulation and experiment show increase in the settling times and overshoots for both links with increasing payload. Similarly for the deflection responses, the simulation algorithm shows similar characteristics as the actual system where the magnitudes of deflections increase with increasing

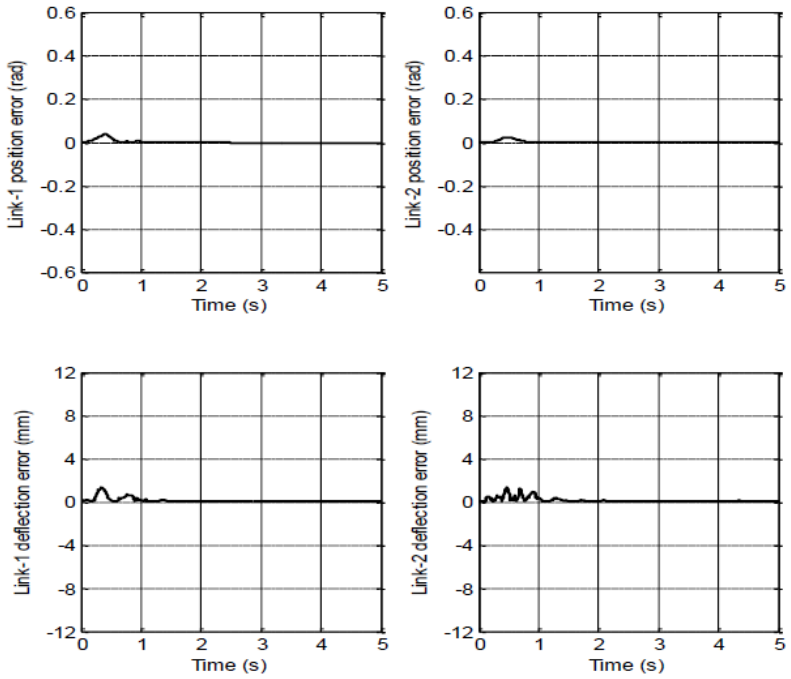

Fig. 15 Error between simulation and experimental results for the system with 0.05 kg payload

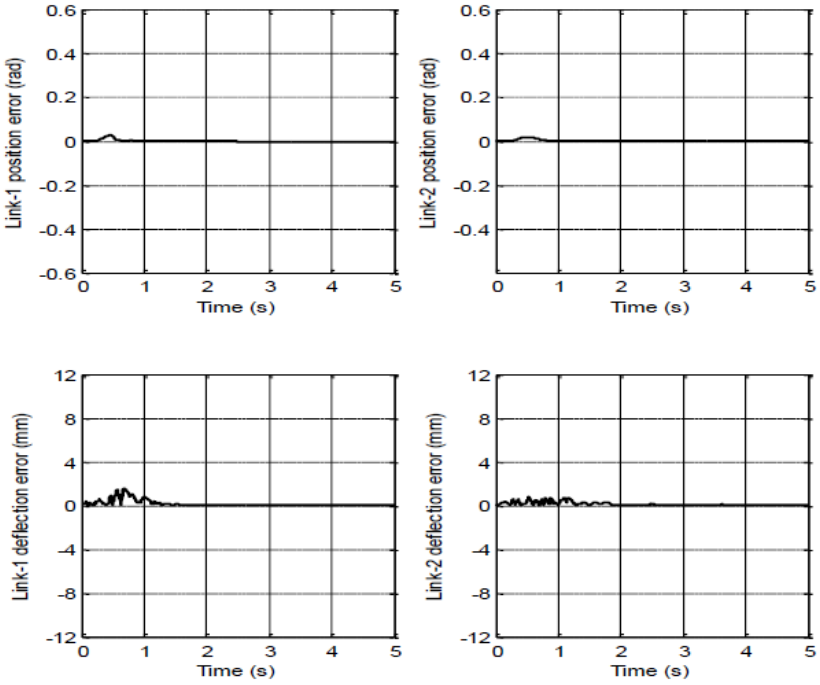

Fig. 16 Error between simulation and experimental results for the system with 0.1 kg payload

payload. Errors between the simulation and experimental results of the responses with payloads of 0.05 kg and 0.1 kg are shown in Figs. 15 and 16 respectively. The errors can be considered negligibly small and thus further reveal the accuracy of the dynamic model.

Comparisons of the resonance frequencies of the system with payloads of 0.05 kg and 0.1 kg obtained with simulations and experiments are shown in Table 3. For the system with a payload of 0.05 kg, relative errors for link-1 are 26% and 6.4% for mode 1 and mode 2 respectively, and for link-2 as 12.4% and 7.4%. For the system with a payload of 0.1 kg, the relative errors for link-1 are 0% and 6.2% for mode 1 and mode 2 respectively, and for link-2 as 0% and 15.3%. Despite a slight difference between the simulation and experimental results, the simulation algorithm provides a good prediction of the behaviour of the experimental rig where the resonance frequencies of the system shift to lower frequencies with increasing payload. Such characteristic behaviour is important and essential for development of suitable control strategies for a two-link flexible manipulator system.

6. Conclusions

Theoretical and experimental investigations into the dynamic modelling and characterisation of a two-link flexible robot manipulator incorporating payload have been presented. A dynamic model of the manipulator has been developed using the AMM methods. Hub angular position and deflection responses for link-1 and link-2 of the manipulator with and without payload are simulated and analysed in time and frequency domain. Moreover, the effects of payloads on the dynamic behaviour of the system are also investigated. Experiments have been performed on the lab-scaled two-link flexible manipulator for validation of the dynamic model. This has been carried out by comparing the simulation and experimental results in terms of time responses and resonance frequencies. The results show that the developed model provides a good prediction of the dynamic characteristics of the actual two-link flexible manipulator with payload. With increasing payload, the simulation algorithm also shows similar characteristics as the actual systems in terms of time domain specifications and resonance frequencies. Thus, confidence in the accuracy of the model for utilisation in subsequent investigations, at development of control strategies for flexible manipulator systems, has been established.

References

Alam, M.S. and Tokhi, M.O. (2007), "Dynamic modelling of a single-link flexible manipulator system: a particle swarm optimisation approach", *J. Low Freq. Noise V. A.*, **26**, 57-72.

De Luca, A. and Siciliano, B. (1991), "Closed-form dynamic model of planar multi-link lightweight robots", *IEEE T. Syst. Man Cy.*, **21**, 826-839.

Dogan, M. and Istefanopulos, Y. (2007), "Optimal nonlinear controller design for flexible robot manipulators with adaptive internal model", *IEE P. Control Theor. Appl.*, **1**, 770-778.

Dwivedy, S.K. and Eberhard, P. (2006), "Dynamic analysis of flexible manipulators, a literature review", *Mech. Mach. Theory*, **41**, 749-777.

Martins, J.M., Mohamed, Z., Tokhi, M.O., Sa da Costa, J. and Botto, M.A. (2003), "Approaches for dynamic modelling of flexible manipulator systems", *IEE P. Control Theor. Appl.*, **150**, 401-411.

Maxon Motor Ag Corporation (2003), *Maxon 03/04 the leading manufacturer of high precision drives and systems*, Maxon motor Innovation.

Nikolakopoulos, G. and Tzes, A. (2010), "Application of adaptive lattice filters for modal parameter tracking of a single flexible link carrying a shifting payload", *Mech. Syst. Signal Pr.*, **24**, 1338-1348.

Pratiher, B. and Dwivedy, S.K. (2007), "Non-linear dynamics of a flexible single link Cartesian manipulator", *Int. J. Non-Linear Mech.*, **42**, 1062- 1073.

Subudhi, B. and Morris, A.S. (2002), "Dynamic modelling, simulation and control of a manipulator with flexible links and joints", *Robot. Auton. Syst.*, **41**, 257-270.

Tao Fan (2007), "Intelligent model predictive control of flexible link robotic manipulators", PhD Dissertation, University of British Columbia, Canada.

Tokhi, M.O. and Mohamed, Z. (1999), "A finite element approach to dynamic modelling of a flexible robot manipulator: performance evaluation and computational requirements", *Commun. Numer.Method. Eng.*, **15**, 669-676.

Tokyo Sokki Kenkyujo Co. Ltd (1996), *Strain gauge user's guide*, Tokyo Sokki Kenkyujo Co. Ltd, Japan.

Yang, Z. and Sadler, J.P. (1990), "Large-displacement finite element analysis of flexible linkage", *J. Mech. Design*, **112**, 175-182.

Wu, J., Wang, L. and Guan, L. (2013), "A study on the effect of structure parameters on the dynamic characteristics of a PRRRP parallel manipulator", *Nonlinear Dynam.*, **74**, 227-235.

JL